Analysis and Minimization of Power-Transmission Loss in Locally Daisy-Chained Systems by Local Energy Buffering

SEHWAN KIM and PAI H. CHOU, University of California, Irvine

Power-transmission loss can be a severe problem for low-power embedded systems organized in a daisy-chain topology. The loss can be so high that it can result in failure to power the load in the first place. The first contribution of this article is a recursive algorithm for solving the transmission current on each segment of the daisy chain at a given supply voltage. It enables solving not only the transmission loss but also reports infeasible configurations if the voltage is too low. Using this core algorithm, our second contribution is to find energy-efficient configurations that use local energy buffers (LEBs) to eliminate peak load on the bus without relying on high voltage. Experimental results confirm that our proposed techniques significantly reduce the total energy consumption and enable the deployed system to operate for significantly longer.

Categories and Subject Descriptors: B.0 [**Hardware**]: General

General Terms: Design, Performance

Additional Key Words and Phrases: Power distribution, embedded systems, daisy-chaining, power management, sensors, energy storage

ACM Reference Format:
Kim, S. and Chou, P. H. 2013. Analysis and minimization of power-transmission loss in locally daisy-chained systems by local energy buffering. ACM Trans. Des. Autom. Electron. Syst. 18, 3, Article 37 (July 2013), 16 pages.
DOI: http://dx.doi.org/10.1145/2491477.2491481

1. INTRODUCTION

Locally daisy-chained (LDC) embedded systems consist of multiple nodes connected in a chain topology. They represent a class of systems with increasingly important applications, though their power efficiency has not been well studied, especially those that rely on the bus for supply-power delivery.

1.1. Examples of Locally Daisy-Chained (LDC) Embedded Systems

A motivating example is a sensing system for monitoring the health of underground water pipelines. Sensors such as these for vibration, moisture, temperature, and camera may be deployed on, near, or inside the pipes for measuring their response to stimulation or environmental conditions. Multiple instances of a given type of sensor, such as accelerometers, may be needed for measuring the propagation speed of a rupture event. Although wireless sensor networks (WSN) have been proposed for similar purposes elsewhere, radio frequency (RF) signal does not travel through ground beyond

This study was sponsored by the National Institute of Standards and Technology (NIST) grant 080058.
Authors' addresses: S. Kim, Department of Electrical Engineering and Computer Science, University of California, Irvine; email: shawn.kim@uci.edu; Pai H. Chou, Department of Electrical Engineering and Computer Science, University of California, Irvine, CA, and National Tsing Hua University, Hsinchu City, Taiwan.

DOI: http://dx.doi.org/10.1145/2491477.2491481

tens of centimeters, making wired connection necessary. Moreover, sensing and actuation require power, but power is often unavailable at the location where the sensor or actuator must be deployed. An LDC structure for data and power represents a natural, practical solution to all these issues.

Another class of systems that also fits the LDC structure is that based on Power over Ethernet (PoE) [IEEE 2009]. DC power of up to 48 V can be delivered to devices such as IP phones, set-top boxes, and other Internet appliances over the eight-conductor RJ45 cable. PoE is convenient in that it requires only one modular connector, similar to traditional telephone lines. Although Ethernet can also be organized in a star topology using a router, a daisy-chained structure may be more convenient and cost effective due to the lower cabling cost.

1.2. Energy Efficiency of LDC Systems

LDC systems have been motivated mainly by necessity, convenience, and other practical considerations, but unfortunately not by their energy efficiency. It turns out that a great deal of obvious inefficiency in such systems can be identified and removed at the power-transmission level. However, design decisions in such systems have often been made based on experience or intuition rather than systematic quantitative analysis.

For instance, the DuraMote network [Kim et al. 2011] consists of one data aggregator connected to one or more daisy-chained sensing nodes over tens of meters of cable. The aggregator node provides a 12V supply, which can drop down to as low as 6 V by the time it reaches a sensing node. That is a 50% drop in voltage. A typical load current of 100 mA translates into 600 mW of power-transmission loss, which is about as much as half of the power consumption of the sensing node itself. Surprisingly, solutions to power-transmission loss in such a system have not been published to date. Traditional network analyses do not apply, because the load is not expressed in terms of constant resistance but in terms of power, which is a product of voltage and current. Without such a solution, designers have no choice but to rely on empirical measurement to assess the efficiency or feasibility of the given configuration. Unfortunately, by the time the system is ready to be measured, it may be too late or too costly to make changes.

1.3. Contributions

This article makes several contributions: a solution to the power-transmission loss problem and its application to finding feasible and energy-efficient configurations based on local energy buffers (LEBs).

First, we propose a recursive algorithm named Cr( ) that solves for the current on each segment of the daisy chain (i.e., on the transmission line and across the load) for the given supply voltage. This algorithm is important in that, for the first time ever, it enables analysis of power loss in LDC systems without having to rely on measurement of actual systems. In addition to analyzing the efficiency of such systems, the algorithm can also identify infeasible configurations, where the power-transmission loss is so great that it is simply impossible to power the load, even if the supply can drive infinite current. The accuracy of this algorithm has been validated with a real LDC system for water pipe monitoring.

Second, we apply the Cr( ) algorithm to finding configurations that are more energy efficient than the baseline ones by reducing or eliminating peak load using local energy buffers (LEBs). Our technique is applicable to systems where the nodes have known duty cycles. By charging the LEBs during low-load times and drawing power from the LEBs to jointly power the high load, we can keep the bus load nearly constant, thereby effectively eliminating the peak load on the bus. This not only minimizes power-transmission loss, but more importantly, it uncovers lower-energy configurations that were previously infeasible at the same supply voltage.

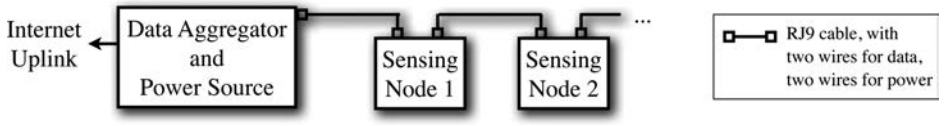

Fig. 1. Daisy-chained water pipeline monitoring system.

Table I. Cable Specification for Power and Data

Cable Type	Conductor (core)	AWG Size	Ampacity (A)	DC Resistance (Ω/km)	Weight
Automotive (12V)	1 (Stranded)	6∼4/0	37∼302	1.296∼0.161	152∼1105kg/km
Power (300/500V)	2 (Stranded)	16∼5	22.8∼5	13.186∼1.027	50∼460kg/km
Coaxial	1 (Solid)	20	13.1	33.29(inner)	39.95kg/km
UTP CAT5	8 (Solid)	24	7.6	< 93.8	23.95kg/km
Telephone	4 (Solid)	24	7.6	< 93.8	11kg/km

** AWG:American Wire Gauge from 50 to 4/0, UTP: Unshielded Twisted Pair

Our proposed tool enables design-space exploration of LDC systems for the very first time. First, it provides exact solutions to the power-transmission loss. Second, it can be used to evaluate feasibility of different configurations and make trade-offs among them in terms of supply voltage and current, capacity of energy storage, daisy-chain length, cable quality (resistance) and price, and duty cycle. Our tool can answer these questions quickly and automatically without requiring the user to build and measure the system.

2. BACKGROUND AND RELATED WORK

This section first presents a case study of the LDC system that motivated this work. Then, we review related work on power distribution and distributed power management.

2.1. Case Study: LDC Sensing System

An example where LDC topology is necessary is a noninvasive water pipe monitoring system from the PipeTECT project [Kim et al. 2011], which falls under the category of tiered, noninvasive remote monitoring systems. The data sampled by the sensor nodes in the sensing tier are transmitted to a node in the data-aggregation tier for evaluation and assessment. The topology is shown in Figure 1. For underground communication between multiple sensing nodes with the data aggregator, we use the controller area network (CAN), a low-complexity, high-throughput wired bus that can support the requirements of real-time monitoring and damage localization of pipes. The robustness of CAN has been proven in the automotive field. Up to 100 nodes can be daisy-chained on the CAN bus, as long as they can all be powered properly.

We use the modular RJ9 jack for corded telephones to enable easy chaining of multiple nodes in the field. An RJ9 cable contains four wires, two of which carry power alongside the other two for CAN data. We call it the *power distribution over CAN* (PDoC). Such an architecture is easy and cost effective to deploy, because one can make a cable of a custom length by simply cutting one of the desired length from a spool and crimping the RJ9 modular connectors on both ends. It can be connected and disconnected easily.

Table I summarizes the specification of various types of cables. For a given cable length, the cross-sectional area of the conductor is inversely proportional to the cable resistance. Therefore, the automotive cable has lower resistance than the others on account of a larger cross-sectional area. However, the cross-sectional area for four conductors is up to 428.8 mm^2, which means the cable can weigh as much as 11.05 kg at 10 m of cable length. The automotive cable is considered too bulky and impractical for

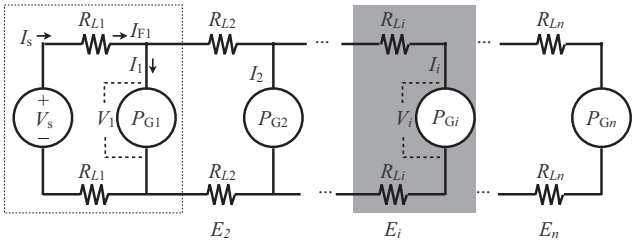

Fig. 2. Equivalent circuit of the daisy-chained power distribution network.

deploying remote sensing systems underground. Instead, the RJ9 cable is desirable or necessary for this application due to ease of deployment, lighter weight, and lower cost.

Note that this daisy-chained setup incurs relatively high power loss when in active mode, due to the resistance in the RJ9 cable and the relatively low supply voltage in the range of 6∼12 V. According to the basic power equation,

$$P = I \times \Delta V = I \times IR = I^2 R, \tag{1}$$

the power loss is quadratically proportional to current I and linearly proportional to resistance R. A high-voltage, low-current combination results in lower power-transmission loss than a low-voltage, high-current one does. However, for DC power, conversion between dissimilar voltages can incur high overhead.

An equivalent-circuit model is important for validation by simulation and power optimization at the power-distribution level. Figure 2 shows the equivalent model of PDoC as a voltage supply (V_s), cable resistance (R_{Li}), and the load of the daisy-chained node (P_{Gi} for $i \in 1 \ldots n$). Note that the load is not constant resistance R_{Gi} but is modeled as (piecewise constant) average power P_{Gi}, where each node may have to trade between V and I.

$$P_{Gi} = V_i \times I_i = \text{constant in a given mode of operation.} \tag{2}$$

The equivalent resistance R_{Gi} would be a function of current, rather than a constant value, because $R_{Gi} \times I_i^2 = P_{Gi}$, where P_{G1} is 1.62 W in active mode, and 15.7 mW in sleep mode, with a small fluctuation.

The DC resistance of a cable directly affects the power-transmission efficiency. For instance, the 12V supply drops down to 11V by the time it reaches a sensing node 5 m away ($R_{\text{cable, 10m}} = 2\Omega$) due to cable resistance, since both the supply and ground rails must be considered. That is an 8.3% drop in voltage to power just one node in active mode attached to the data aggregator, or 42.7 mW of power loss over the power distribution line. As additional daisy-chained nodes are turned on and pull down the bus voltage, the power loss increases superlinearly with the load, because each node pulls even more current to maintain the same power consumption at a lower voltage. The power loss may be so great that it will not be able to deliver enough power beyond a certain point in the daisy chain.

Voltage stacking, also called charge recycling, is one approach to matching high-voltage supply power with low-voltage power consumers by composing them in series. Much work in this area has been done by Intel for saving power on-chip, and the same principle can apply to our distributed structure by reducing the average current I demands by a factor of n [Rajapandian et al. 2006]. However, a push-pull regulator and decoupling capacitance are required to stabilize charge mismatches, which can increase the complexity of the control layer and limit the number of stackable logic blocks. Also, the original voltage stacking assumes power consumers are physically close to each other, but in our setup, the power consumers are far apart and connected by long

power-transmission line segments. Since the voltage drop across each transmission segment scales inversely proportionally with the number of segments and nodes, a voltage-stacked structure is not really less scalable than an LDC.

2.2. DC Power Distribution

DC power-distribution techniques have been used since the very beginning of electric lighting and are increasingly being applied in recent years. Edison advocated DC, which could be stored in batteries, but AC won for utility power due to easy voltage transformation and efficient transmission. DC power has been in wide use for garden lighting and sprinkler systems for many decades, and recent years have seen increasing use of DC in data centers [Ton et al. 2008], electric vehicles [Chan 2002], shipboard systems [Ciezki and Ashton 2000], photovoltaic systems [Yang et al. 2010], and fuel cells [Wolk 1999]. Deeply deployed sensing systems [Kim et al. 2011; Whittle et al. 2010] use DC power-distribution techniques to address the difficulty in replacing batteries underground. The cluster head above ground has access to either utility power or an energy harvester in conjunction with an energy storage element (ESE), and it distributes DC power to the underground sensing nodes. Whittle et al. [2010] employed one ESE to power one sensing node, while Kim et al. [2011] uses one ESE that powers multiple daisy-chained sensing nodes, but the nodes themselves do not store energy. However, since the previous power-distribution techniques did not consider the power-transmission loss caused by the cable resistance, they suffer from low energy efficiency.

2.3. Power Management over LDC

Literature in low-power design commonly classifies power management techniques into dynamic voltage/frequency scaling (DVFS) and dynamic power management (DPM). DVFS reduces supply voltage to achieve quadratic power reduction. It is allowed to do so when slack time is available or if parallelism is effective. DPM, on the other hand, puts idle peripheral devices into power-saving or shutdown mode when they are not used by ensuring that the overhead due to mode switching does not exceed the energy savings. All of these techniques can be applied to both the sensing and data-aggregation subsystems of the water pipe monitoring network individually. However, the more important issues here are (1) coordinated power management of the nodes and (2) power management of the supply rails and power distribution scheme.

Coordinated distributed power management (CDPM) has been proposed [Zamora and Marculescu 2007] for wireless video sensor networks. The purpose is to allow each node to make its own policy decisions while considering its neighbor's traffic load with predictive wakeup. The nodes carry their own power sources individually and rely on the same wireless data link and timeout for coordination but without power transmission. Others propose middleware for coordinating power-management decisions [Nathuji 2008], though they assume compute-dominated workload and do not consider the cost of the communication link. Coordinated power management has also been proposed for chip multiprocessors [Devadas and Aydin 2010], but it is centralized and does not consider the communication cost or power distribution, either.

Unlike the CDPM structures, we propose an efficient power-distribution technique with optimal scheduling of powering the nodes and charging and discharging their LEBs. The introduced LEBs help minimize power-transmission loss by eliminating peak transmission current.

3. ALGORITHM FOR ANALYSIS AND OPTIMIZATION OF LDC SYSTEM

We define the optimization problem as follows: given an LDC of nodes, each with its own load at a given duty cycle and the cable resistance of each segment, choose the right voltage-current combination to power the nodes while minimizing power-transmission

loss. We first show that power-transmission loss is minimized when the bus current is kept constant (i.e., average level) for the entire time. Constant bus load can be achieved by a hybrid power system consisting of the power-transmission bus and a local energy buffer (LEB) on each sensing node.

This section first proves optimality of constant bus load. No closed-form solutions to power-transmission loss have been published, and here we use a recursive algorithm named Cr( ) to solve for the current in active and sleep modes. Then, we apply the Cr( ) algorithm to determine the load to draw from each power source in the bus-LEB hybrid power system. This entails scaling the power by the given duty cycle to determine the target constant bus-power level to maintain.

3.1. Optimality of the Constant Bus Current

We sketch a simple proof that the constant bus current is optimal for minimizing power-transmission loss. To show why this is the case, consider an average current of $\bar{I}$ and fluctuation by $\pm\Delta I$.

$$\begin{aligned} P_{\text{loss}} &\propto \left(\bar{I}-\Delta I\right)^2+\left(\bar{I}+\Delta I\right)^2=\bar{I}^2-2\bar{I}\,\Delta I+\Delta I^2+\bar{I}^2+2\bar{I}\,\Delta I+\Delta I^2 \\ &= 2\bar{I}^2+2\Delta I^2 \;>\; 2\bar{I}^2 \text{ if } \Delta I\neq 0, \end{aligned} \tag{3}$$

that is, any fluctuation in current when delivering the same amount of energy within the same duration results in additional power loss that is proportional to the square of the fluctuation current (ΔI^2). With the hybrid bus-LEB power, during times of low load, the surplus bus power can be used to charge the LEB, and during times of high load, the LEB can jointly power the load with the bus by the deficit amount.

3.2. Voltage-Current Solution in LDC Power Transmission

The load power is a product of voltage and current. More specifically, given the voltage, the load power responds by drawing the amount of current that it needs for the load. Solving DC power-transmission loss is equivalent to solving for the transmission current at a given supply voltage. The power-transmission loss in an LDC network has a closed-form solution for a one-node case (i.e., the subcircuit in the dotted box in Figure 2 with load P_{G1}) based on the following quadratic formula.

$$I_1=I_s=\begin{cases}\frac{P_{\text{G1}}}{V_s}, & \text{if } R_{\text{L1}}=0,\\ \frac{V_s-\sqrt{V_s^2-8R_{\text{L1}}P_{\text{G1}}}}{4R_{\text{L1}}}, & \text{otherwise.}\end{cases} \tag{4}$$

However, the problem has no known closed-form solution for two or more nodes. Instead, the loss can be solved iteratively or recursively. A recursive solution we use is shown in Algorithm 1, which decomposes an LDC circuit into stages. It alternates between pulling down the voltage to the ith-stage circuit and to the (recursive) $(i+1)$th...nth chain until they converge. The base solution assumes ideal dc-dc converters (i.e., 100% efficiency). Cr( ) will converge because the V_i or I_i will increase monotonically or at most stay flat based on constant P_{G}. The voltage and current combination of each daisy-chained node can be found recursively by calling Cr( ) and recording the results using a matrix. If the voltage is not sufficiently high to power the load, then the quadratic formula will fail while attempting to take the square root of a negative quantity. The algorithm catches this condition in the try-catch block (lines 4–8).

3.3. Constant-Current Optimization

Given the algorithm for solving the currents on all LDC segments, we use it to find the constant bus current that minimizes power-transmission loss. Before we state the algorithm, we define the two baselines and our proposed case.

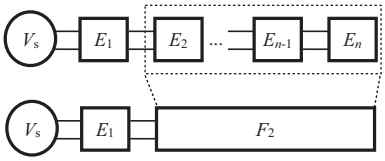

Fig. 3. Notation for subcircuits: E_i is the subcircuit of each stage, while F_i is the concatenation of subcircuits $\mathrm{E}_i \ldots \mathrm{E}_n$.

ALGORITHM 1: $\mathrm{Cr}(i, P_\mathrm{G}, R_\mathrm{L})$ – Solving Current Recursively

Input: i, where V_{i-1} is the apparent supply voltage; $P_{\mathrm{G}1\ldots n}$ the power consumption of each node; $R_{\mathrm{L}1\ldots n}$ the transmission-line resistance of each segment.
Output: $I_{\mathrm{F}i}$, the cumulative current consumption of $\mathrm{E}_i \ldots \mathrm{E}_n$, where E_i = sub-circuits in gray box in Figure 2, and F_i is the concatenation of $\mathrm{E}_i \ldots \mathrm{E}_n$ as shown in Figure 3.

if $i > n$ **then** // *base case, beyond last stage*
  return 0;
end
try:
  $I_i \leftarrow \begin{cases} \frac{P_{\mathrm{G}i}}{V_{i-1}} & \text{if } R_{\mathrm{L}i} = 0, \\ \frac{V_{i-1} - \sqrt{V_{i-1}^2 - 8R_{\mathrm{L}i}P_{\mathrm{G}i}}}{4R_{\mathrm{L}i}} & \text{otherwise} \end{cases}$; // *quadratic formula on* E_1
catch *exception attempting to take square root of a negative number*
  report error: "insufficient voltage to power the load";
end
$V_i \leftarrow \frac{P_{\mathrm{G}i}}{I_i}$; // *Voltage across* G_i*, which is the perceived supply voltage to* F_{i+1}
while *True* **do** // *could break after some number of iterations*
  $I_{\mathrm{F}i} \leftarrow I_i + \mathrm{Cr}(i+1, P_\mathrm{G}, R_\mathrm{L})$; // *combine recursive result*
  $V_i' \leftarrow V_{i-1} - 2R_{\mathrm{L}i}I_{\mathrm{F}i}$; // *check impact of* F_{i+1} *on* V_i
  if $V_i = V_i'$ **then** // *alternatively,* $V_i - V_i' < \epsilon$
    return $I_{\mathrm{F}i}$;
  end
  $V_i \leftarrow V_i'$;
  $I_i \leftarrow \frac{P_{\mathrm{G}i}}{V_i}$; // *refresh using the now lower* V_i'
end

Baseline 1: No Power Management, No LEB. The first baseline system is the daisy-chained system, that is, powered entirely by the bus without any power management. The solution to the power loss on each segment i (one for the supply rail and one for the ground rail) is simply $I_{\mathrm{F}i}^2 R_{\mathrm{L}i}$, where $I_{\mathrm{F}i}$ is the output of $\mathrm{Cr}(i, P_\mathrm{G}, R_\mathrm{L})$, as in Algorithm 1.

Baseline 2: Duty-Cycled, No LEB. The second baseline system is the same daisy-chained system still powered entirely by the bus but power managed with an equivalent duty cycle (see Figure 4). That is, the system can be viewed as switching between active and low-power modes either on a regular basis or by event triggering but upper-bounded by the fraction of time it operates in active mode.

Proposed Case: Duty-Cycled, Hybrid Bus-LEB Power. Our proposed case assumes the same power-managed load as in Baseline 2, but we modify the hardware by adding an LEB to each node. The idea with our optimization algorithm is to keep the load on the bus constant, which would minimize the transmission loss. During low load (i.e., sleep mode), the bus power is used to charge the LEBs; during high load (i.e., active mode),

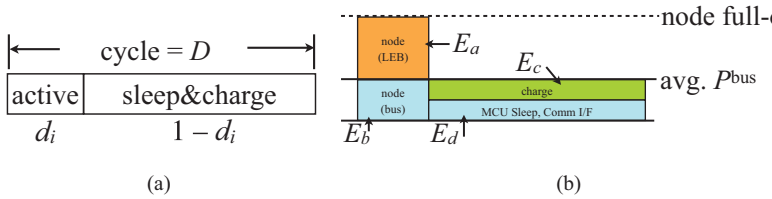

Fig. 4. Energy and power breakdown in a duty cycle.

the LEB and the bus jointly power the node such that the bus load is kept constant the entire time.

We define the following variables.

—D duty period (i.e., length of one period).
—d_i duty cycle of node i (i.e., fraction of time it spends in active mode).
—E_a, P_a. Energy and power contributed by LEB to power the node (implicitly i for the rest of the symbols defined in this group) during active mode.
—E_b, P_b. Energy and power contributed by the bus to power the node during active mode ("b" for "bus").
—E_c, P_c. Energy and power contributed by the bus during sleep-and-charging mode to charge the LEB ("c" for "charging").
—E_d, P_d. Energy and power contributed by the bus during sleep-and-charging mode to power the node (MCU sleep, but communication interface on).

Note that we use the (italicized) symbols $E_a, E_b, \ldots$ for energy and (unitalicized) $\mathrm{E}_1, \mathrm{E}_2, \ldots$ for subcircuits in a daisy chain. The contexts are entirely different, so the overloading of notation should cause no confusion. With implicit suffix i, our goal is to solve for P_b given P_G, P_d, D, and d. Then, P_a and P_c can be expressed in terms of P_b. The following equalities and inequalities must hold.

$$P_b \geq P_\mathrm{G} \cdot d + P_d \cdot (1 - d); \tag{5}$$
$$P_a = P_\mathrm{G} - P_b; \tag{6}$$
$$P_c = P_b - P_d. \tag{7}$$

In the general LDC, the current on each transmission line segment can be solved by calling the same Cr( ) algorithm as before, except every $P_{\mathrm{G}i}$ is replaced with the corresponding P_{bi}.

For illustration, consider the one-node example where $P_\mathrm{G} = 1.5\mathrm{W}$, $P_d = 25\mathrm{mW}$, $D = 60\mathrm{s}$, $d = 5\%$, $R_\mathrm{L} = 1\Omega$ (one for the supply and one for the ground). The power consumptions of the three schemes are as follows.

Scheme	P_b (mW)	E_b (J)	I@6V (mA)	E^{loss}@6V (mJ)		I@3V	E^{loss}@3V (mJ)	
Baseline 1	1500	90.00	275.26	9092		infeas.	infeasible	
Baseline 2 active	1500	4.50	275.26	454.59	456.58	infeas.	infeas.	infeas.
Baseline 2 sleep	25.00	1.425	4.172	1.985		8.380	8.01	
LEB	98.75	5.93	16.55	32.87		33.67	136.06	

As this example shows, Baseline 2 may use significantly lower energy than Baseline 1 (4.5 J vs. 90 J), but they have the same peak power. The problem is that it must be operated at above 3 V as its minimum voltage, or else the transmission loss is so high that it cannot deliver sufficient power to the node. In other words, both Baseline 1 and Baseline 2 will fail to operate (at least during active period) when the supply voltage drops below 4 V. On the other hand, our proposed scheme draws either 16.55 mA at

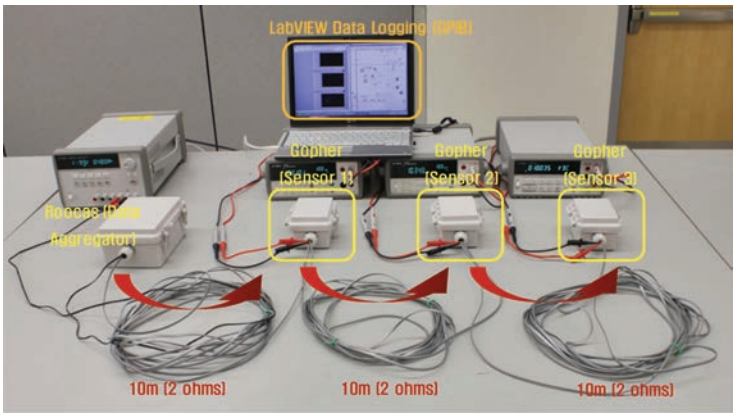

Fig. 5. Experimental setup for power distribution over CAN.

6 V or 33.67 mA at 3 V minimum. Not only is the energy loss of our LEB scheme significantly lower (136.06 mJ at 3V vs. 456.58 mJ of Baseline 2 at 6 V), it is actually feasible at half the supply voltage.

With LEBs, because all nodes appear to maintain a constant load to the bus regardless of their mode of operation, the nodes can manage their own power independently without any synchronization. The schematic for the LEB power-sharing circuitry is shown in Figure 6 the next section.

4. EXPERIMENTAL RESULTS

The experiments serve two purposes: (1) to show the effectiveness of our proposed LEB scheme compared to the Baseline schemes by measurement on a real system and (2) to demonstrate applicability of the Cr( ) algorithm to the design-space exploration of LDC systems. This section first describes the experimental setup for the three schemes being compared. We validate the correctness and evaluate the accuracy of the Cr( ) algorithm by comparing its output with measurement results over these schemes. Then, we show results generated over a range of supply-voltage values as an example use of our algorithm for design-space exploration. Other parameters, such as duty cycle, LDC length, and LEB capacity, can also be swept similarly.

4.1. Experimental Setup

4.1.1. Hardware. Our experimental setup consists of one data aggregator and three daisy-chained sensing nodes, as shown in Figure 5. Adjacent nodes are connected via a 10m phone cable (RJ9) with four wires of $R_{Li} = 1\Omega$ each, including one for supply, one for ground, and two for CAN data. The voltage and current are measured at the intake of each node using a digital multimeter (Agilent 34405A), with resolutions of 10μA and 1 mV. The daisy chain is powered by a regulated 12V supply (Agilent E3631A, with 1 mA resolution) and consists of three identical sensing nodes. Although the data aggregator also consumes power, it is not counted as part of the daisy chain for the purpose of this experiment. The data aggregator is responsible for controlling the distribution of power to these three daisy-chained sensing nodes. The power consumption of each node is $P_{Gi}^{\text{active}} = 1.62$ W in active mode and $P_{Gi}^{\text{sleep}} = 15.7$ mW in sleep mode. There is no inherent difficulty with incorporating the data aggregator or heterogeneous loads, as our algorithm is general and can handle any combination of loads in daisy chains of any length. The schematic of the LEB for our experiment is shown in Figure 6. We use

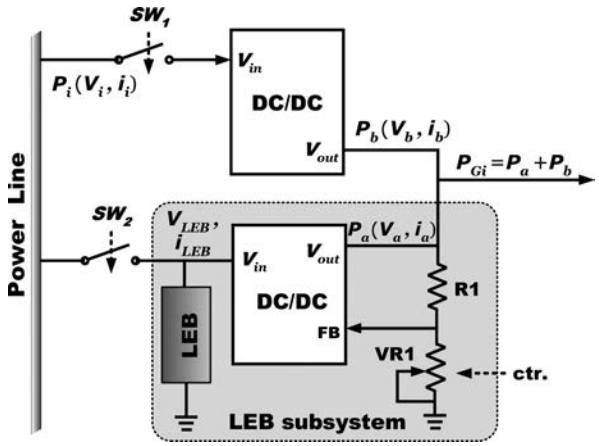

Fig. 6. Power-sharing circuitry and LEB subsystem.

a supercapacitor, which can support the kind of power density needed without the kind of aging effect seen with batteries.

4.1.2. Baseline 1: 100% Active, No LEB. For Baseline 1, the sensing system is configured to use only active mode the entire time. This is the most conservative setup and is used when the domain expert (civil engineer in this case) wants the entire raw data. Each sensing node consumes 1.62 W at the sampling rate of 1.2 ksps and data speed of 1 Mbps on the CAN bus.

4.1.3. Baseline 2: Duty-Cycled, No LEB. To achieve duty-cycled operation, the sensing nodes are programmed to switch between active and sleep modes. In sleep mode, our sensing node consumes 15.7 mW by turning off other peripheral devices while keeping the CAN transceiver on to accept incoming messages. Regardless of modes, one data aggregator supplies power to all LDC sensing nodes. The required data-acquisition frequency is 36 times per day, based on previous studies that measured the natural frequency-response range of cable-stayed bridges from 0.5 Hz to 15 Hz [Rice et al. 2010]. In our experiment, therefore, the minimum target frequency is set up to be 0.1 Hz, which is suitable to monitor most civil infrastructure systems. It takes 60 seconds to detect the minimum frequency response of the target civil structures. As a result, one cycle is composed of 60 seconds in active mode and 2,340 seconds in sleep mode, for a total of 2,400 seconds.

4.1.4. Proposed Scheme: Duty-Cycled, Hybrid Bus-LEB Power. Our proposed scheme, referred to as the LEB scheme, assumes the same duty cycle as Baseline 2, except that it uses an LEB to eliminate the peak power. The LEBs for all nodes are fully charged before the experiment. When in active mode, each node operates in power-sharing mode by drawing power from both the bus and the LEB to jointly drive the load. When in sleep mode, each node operates in sleep-and-charging mode by using the bus power to drive the node in sleep mode and to charge the LEB. The power-sharing (PS) factor is defined as the ratio of power contribution of the LEB to the load,

$$\text{PS factor} = \frac{P_a}{P_{\text{G}} = P_a + P_b}, \tag{8}$$

and the sleep-charging ratios are determined using the equations presented in Section 3.3. The LEB subsystem is equipped with an adjustable dc-dc converter. The output voltage of the converter can be adjusted by an external resistive voltage divider.

Table II. Measured Voltage, Current, and Power-Transmission Loss at each LDC segment in Each Mode

Scheme	Mode	Measured	G1	G2	G3	E_{loss}(mode)	E_{loss} total
Baseline 1	Active	Voltage (V_i)	11.08 V	10.45 V	10.13 V	100% active	1620.36J
		Current ($I_{\text{F}i}$)	461.2 mA	315.1 mA	159.9 mA		
		Power ($P_i^{\text{tr.loss}}$)	425.41 mW	198.58 mW	51.16 mW	2.5% active, 97.5% sleep	40.51J + 0.1229J = 40.622 J
Baseline 2	Sleep	V_i	11.99 V	11.99 V	11.98 V		
		$I_{\text{F}i}$	3.934 mA	2.623 mA	1.311 mA		
		$P_i^{\text{tr.loss}}$	31.0 μW	13.8 μW	3.44 μW		
LEB	Power Sharing	V_i	11.58V	11.3V	11.18V	2.5% power sharing, 97.5% sleep & charging	8.693J + 8.424J = 17.12J (1.465J lower bound)
		$I_{\text{F}i}$	214.8mA	144.83mA	72.9mA		
		$P_i^{\text{tr.loss}}$	92.28mW	41.95mW	10.65mW		
	Sleep and Charging	V_i	11.93V	11.89V	11.86V		
		$I_{\text{F}i}$	33.97mA	22.65mA	11.33mA		
		$P_i^{\text{tr.loss}}$	2.31mW	1.03mW	0.26mW		

To automatically control the PS factor, we modified the feedback circuit to the dc-dc converter by replacing one of the resistors of the voltage-divider network with a digital potentiometer (VR1), as shown in Figure 6.

4.2. Measurement Results

We measured the voltage drop (i.e., V_i) across node i and the current on the power segment (i.e., $I_{\text{F}i}$) from node $i-1$ to i. The power-transmission loss of each node in every scheme can be calculated by multiplying its measured current and voltage, as shown in Table II. The energy loss is derived by multiplying the power by the time spent in each mode within the cycle of 2,400 seconds.

4.2.1. Power-Transmission Loss. The Baseline-1 scheme runs in active mode the entire time, and the total power-transmission loss is $P_{\text{total}}^{\text{tr.loss}} = 675.15$ mW, or around 41% of the power consumption of one sensing node in active mode. This severely limits the operational time and the length of the daisy chain. Although theoretically the CAN bus can connect up to 100 nodes, such power-transmission loss will be a crucial factor in determining the actual maximum number of daisy-chained nodes.

One technique to reduce the power loss is the Baseline-2 scheme, which duty-cycles active mode at 2.5% while spending the rest of the time in sleep mode. However, since the Baseline-2 scheme does not eliminate the peak transmission current, its peak power-transmission loss is identical to that of Baseline-1, even though its average power is much lower. This implies that the feasibility of such an LDC operating at a given voltage is considered identical to that of Baseline-1. Although one may attempt to reduce the peak by a factor of n by scheduling at most one active node at a time, doing so will not work in this particular application, as discussed in Section 4.4.2.

Differing from both Baseline schemes, our LEB scheme can mitigate or remove the peak load by the power-sharing technique. Although the power-transmission loss of LEB in sleep-and-charging mode is higher than that of Baseline-2 in sleep mode, it is much smaller compared to the peak transmission current in active mode. In this experiment, we swept the PS factor that resulted in the $P_{\text{total}}^{\text{tr.loss}} = 144.88$mW in active mode. Table II shows the results of measured current and voltage using the baseline schemes in both active and sleep modes and the proposed scheme.

4.2.2. Energy-Transmission Loss. The Baseline-2 scheme cuts the energy loss of Baseline-1 from 1620.36 J down to 40.622 J, or by a factor of 40. Not only is this tremendous in terms of the energy ratio but also significant on an absolute scale.

Table III. Measured Voltage and Current in Power Sharing Mode@$V_i = 12$V, $V_{LEB} = 2.4$V

PS factor $= P_a/P_{\mathrm{G}}$	V_a	I_a	V_b	I_b	I_a+I_b	V_G
0.00482	4.70V	1.66mA	5V	325.4mA	327.06mA	4.953V
0.01211	4.75V	4.13mA	5V	322.7mA	326.83mA	4.957V
0.02993	4.80V	10.1mA	5V	316.6mA	326.68mA	4.959V
0.07021	4.85V	23.45mA	5V	303.1mA	326.52mA	4.961V
0.1558	4.90V	51.5mA	5V	274.8mA	326.33mA	4.964V
0.3025	4.95V	99.0mA	5V	226.5mA	325.53mA	4.976V
0.5000	5.00V	161.9mA	5V	161.9mA	323.81mA	5.000V
0.6996	5.05V	224.4mA	5V	98.0mA	322.43mA	5.024V
0.8487	5.10V	269.6mA	5V	50.4mA	320.03mA	5.062V
0.9340	5.15V	293.8mA	5V	23.8mA	317.64mA	5.100V
0.9764	5.20V	304.2mA	5V	9.63mA	313.83mA	5.162V
0.9959	5.25V	307.3mA	5V	3.90mA	311.19mA	5.206V
1.0119	5.30V	309.3mA	5V	1.37mA	307.65mA	5.266V

Note: PS factor is the ratio of LEB power contribution P_a to total node load (P_{G}).

Every hour, the power-transmission loss is equivalent to draining over half of a typical cell-phone battery, even when the sensing nodes are run at only 2.5% duty cycle.

Table II also shows the summary of energy loss comparison between both Baseline schemes and the proposed LEB scheme. Our LEB scheme further reduces the energy-transmission loss to 17.12 J at a 50% PS factor under the same duty-cycle condition of Baseline 2. Compared to Baseline 1, our LEB scheme is able to decrease the energy loss by a factor of 95. Our optimal solution, that is, Eq. (5) prescribes for each node the average load to draw from the bus.

$$\begin{aligned} P_b &\geq P_{\mathrm{G}} \cdot d + P_d \cdot (1-d) \\ &= 1.62\mathrm{W} \times 0.025 + 15.7\mathrm{mW} \times 0.975 \\ &= 55.8\mathrm{mW}. \end{aligned} \tag{9}$$

Since we have three identical nodes, they have the same average load. This means each LEB must contribute $1.62\mathrm{W} - 55.8\mathrm{mW} = 1.5642\mathrm{W}$ of power during active mode, or 96.56%, while the bus contributes 3.44% during active mode. This PS factor yields the energy-transmission loss of merely 1.465 J as the theoretical lower bound. The measured result is 17.12 J total for all three nodes because the overhead of the LEB circuitry, as depicted in Figure 6. We measure its voltage and current in power-sharing mode (i.e., $SW1$ and $SW2$ are on) separately at the power line voltage of 12V and LEB voltage of 2.4V, and the results are shown in Table III. As the PS factor increases, an intermediate voltage (V_G) rises, while the load current decreases to maintain the constant P_{G}. Table III shows the measured voltage and power over the range of operating conditions from nearly 0 to over 100% contribution by the bus to each P_{G}. The LEB circuit can cover a complete range of target PS factors.

4.3. Design-Space Exploration by Voltage Sweeping

Our Cr() algorithm and the equations for LEB power optimization can be a powerful tool for design-space exploration. An example is shown in Figure 7, where the designer may want to see the trends in power and energy losses over different supply voltages. Our system implementation currently works with a fixed 12V supply, but it would be useful to know how severe the losses may be at other supply voltages without having to build a system to work at so many different levels.

Tables IV to VI show the voltage, current, and power-transmission loss of the daisy chain as calculated by our Cr( ) algorithm over supply voltages from 18 V down to 3 V

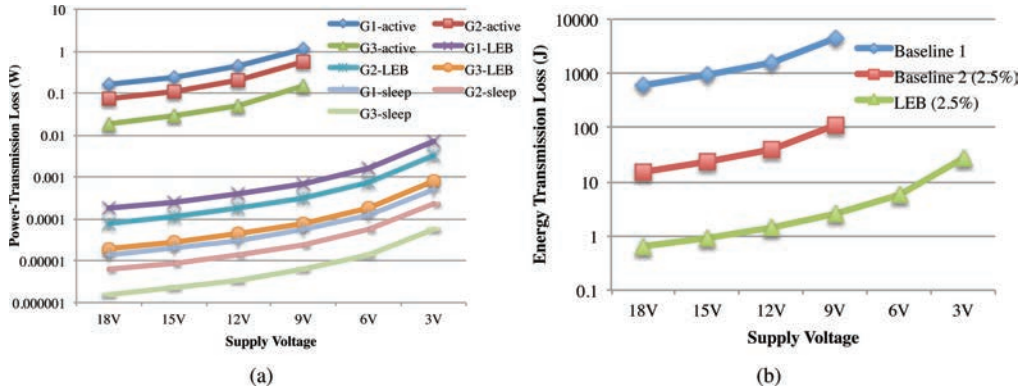

Fig. 7. (a) Power-transmission loss vs. supply voltage at each node (G1–G3) in each mode; (b) total energy-transmission loss of the entire daisy chain. Note that in active mode (which is used by both Baseline 1 and Baseline 2), 6V and 3V are infeasible.

Table IV. Voltage, Current, and Transmission Loss Computed by Cr() Algorithm at Supply Voltages 18 V and 15 V

Mode	Computed	G1	G2	G3	Mode	Computed	G1	G2	G3
Active	V_i	17.43V	17.05V	16.86V	Active	V_i	14.30V	13.83V	13.59V
	I_{Fi}	284.05mA	191.12mA	96.10mA		I_{Fi}	349.64 mA	236.36 mA	119.21 mA
	$P_i^{\text{tr.loss}}$	161.37mW	73.05mW	18.47mW		$P_i^{\text{tr.loss}}$	244.50 mW	111.73 mW	28.42 mW
Sleep	V_i	17.99V	17.99V	17.99V	Sleep	V_i	14.99V	14.99V	14.99V
	I_{Fi}	2.62mA	1.75mA	872.73μA		I_{Fi}	3.14mA	2.09mA	1.05mA
	$P_i^{\text{tr.loss}}$	13.71μW	6.09μW	1.52μW		$P_i^{\text{tr.loss}}$	19.74μW	8.78μW	2.19μW
LEB	V_i	17.98V	17.97V	17.96V	LEB	V_i	14.98V	14.96V	14.96V
	I_{Fi}	9.32mA	6.21mA	3.11mA		I_{Fi}	11.19mA	7.46mA	3.73mA
	$P_i^{\text{tr.loss}}$	173.59μW	77.19μW	19.31μW		$P_i^{\text{tr.loss}}$	250.32μW	111.35μW	27.85μW

Note: "LEB mode" is short for both power-sharing and sleep-and-charging modes, which ideally consume identical amounts of power from the bus.

Table V. Voltage, Current, and Transmission Loss Computed by Cr() Algorithm at Supply Voltages 12 V and 9 V

Mode	Computed	G1	G2	G3	Mode	Computed	G1	G2	G3
Active	V_i	11.08V	10.45V	10.13V	Active	V_i	7.52V	6.48V	5.93V
	I_{Fi}	461.27mA	315.02mA	159.96mA		I_{Fi}	738.73mA	523.38mA	273.22mA
	$P_i^{\text{tr.loss}}$	425.53mW	198.48mW	51.17mW		$P_i^{\text{tr.loss}}$	1.09W	547.86mW	149.30mW
Sleep	V_i	11.99V	11.99V	11.98V	Sleep	V_i	8.99V	8.98V	8.98V
	I_{Fi}	3.93mA	2.62mA	1.31mA		I_{Fi}	5.24mA	3.50mA	1.75mA
	$P_i^{\text{tr.loss}}$	30.87μW	13.73μW	3.43μW		$P_i^{\text{tr.loss}}$	54.97μW	24.45μW	6.11μW
LEB	V_i	11.97V	11.95V	11.94V	LEB	V_i	8.96V	8.94V	8.93V
	I_{Fi}	14.00mA	9.34mA	4.67mA		I_{Fi}	18.72mA	12.50mA	6.25mA
	$P_i^{\text{tr.loss}}$	392.15μW	174.52μW	43.66μW		$P_i^{\text{tr.loss}}$	701.16μW	312.35μW	78.20μW

in 3 V decrements. This is an example use of our tool for design-space exploration. First, our calculated results in the left subtable of Table V (12V supply) match the measurement results shown in Table II very accurately, to within 0.1%. The only place where they differ is when the power is very low such that other effects, such as the overhead of dc-dc converters and limit on instrument resolution, start to dominate. Other than that, one could use this tool to ask what-if questions before actually building or revising the system, which can be a time-consuming task. In addition to the questions

Table VI. Voltage, Current, and Transmission Loss Computed by Cr() Algorithm at Supply Voltages 6 V and 3 V

Mode	Computed	G1	G2	G3	Mode	Computed	G1	G2	G3
Active	V_i	5.40V	3.35V	failed	Active	V_i	failed	failed	failed
	$I_{\mathrm{F}i}$	738.73mA	1.03A	failed		$I_{\mathrm{F}i}$	failed	failed	failed
	$P_i^{\mathrm{tr.loss}}$	1.09W	2.11W	failed		$P_i^{\mathrm{tr.loss}}$	failed	failed	failed
Sleep	V_i	5.98V	5.97V	5.97V	Sleep	V_i	2.97V	2.95V	2.94V
	$I_{\mathrm{F}i}$	7.88mA	5.26mA	2.63mA		$I_{\mathrm{F}i}$	15.96mA	10.68mA	5.35mA
	$P_i^{\mathrm{tr.loss}}$	124.26μW	55.31μW	13.84μW		$P_i^{\mathrm{tr.loss}}$	509.76μW	227.93μW	57.19μW
LEB	V_i	5.94V	5.91V	5.89V	LEB	V_i	2.88V	2.80V	2.76V
	$I_{\mathrm{F}i}$	28.32mA	18.93mA	9.48mA		$I_{\mathrm{F}i}$	59.52mA	40.14mA	20.22mA
	$P_i^{\mathrm{tr.loss}}$	1.60mW	716.74μW	179.76μW		$P_i^{\mathrm{tr.loss}}$	7.08mW	3.22mW	817.56μW

Note: The results for G1 and G2 in active mode are where the algorithm stops when it finds G3 infeasible, not the actual solution.

on power-transmission loss, one could also ask questions such as "How low can the supply voltage be?" "How long can the daisy chain be before the system starts failing?" One can see that the system can work down to 9 V for all schemes. Further lowering of the supply voltage down to 6 V and 3 V will cause both Baselines 1 and 2 to fail. The reason Baseline 2 also fails is that its peak power is identical to that of Baseline 1. On the other hand, our LEB scheme continues working even when the supply is as low as 3 V. This type of precise analysis was not possible previously without our tool.

4.4. Discussion

Several issues require further discussion. They include (1) leakage, resolution, and efficiency of the LEB and (2) peak-load power management policies.

4.4.1. Leakage, Resolution, and Efficiency of LEB. One issue with the LEB is how precisely one can control the power contributions by the bus and LEB in charge-sharing mode. That is, after computing the amount of average bus power to draw, we can then set the control voltage (VR1) in Figure 6 accordingly. The bus load is supposed to be a constant and is known prior to deployment. If this assumption holds, then this circuit can work well. However, the VR1 is usually digitally controlled with limited resolution in that it will not output precisely the intended amount of power. As Table III shows, the control voltage is not on a linear scale. The resolution increases towards the extremes (i.e., 0% or 100%), and fortunately, that matches our operating region well (2.5% from the bus). In general, it is a good idea to overengineer the system and be conservative by budgeting slightly more power from the bus and potentially less from the LEB so that the LEB will not run out of energy when needed. Although LEBs are leaky, especially if they are supercapacitor-based, we assume that (1) we do not charge them up to the exponential-growing leakage region, and (2) the duty period is not too long compared to the leakage rate. Given that it is common for supercapacitor-based systems to operate at leakage levels on the order of μA, a duty period of 40 minutes translates into leakage energy of a few joules, which is quite acceptable.

Another consideration is the round-trip efficiency of the supercapacitor or battery, or the ratio of usable energy to charged energy. Even without considering the leakage, supercapacitors have the issue of unusable residual charge, or the amount of charge below the minimum usable voltage. When sizing the supercapacitor and computing the round-trip efficiency, the residual energy should be subtracted from the total capacity. The charging budget can be scaled accordingly. In practice, this overhead comprises a very small amount compared to the power-transmission loss [Kim and Chou 2012].

The LEB circuitry includes dc-dc converters, which usually have a minimum voltage of 0.7 V. When working with supercapacitor-based storage, most of the time, the dc-dc

converter will operate in boost mode, and the loss should be considered. Most dc-dc converters have a quiescent current (i.e., minimum current draw when load is zero) of 1–2 mA, though this overhead can be absorbed into a higher load. Recent advances in hysteretic converters can bring the quiescent current down to about 1 μA.

4.4.2. Peak Load and Power Management. One might ask if we intentionally made Baseline 2 look worse than it needs to be by considering simultaneous peaks. If we are allowed to space apart the peak power draw by different nodes, then we can cut the worst-case peak by a factor of n, where n is the number of nodes in the system. However, in the general case, the worst-case must still be considered. Either they do not synchronize, which means they can power manage independently and can be active simultaneously, or they perform (clock) synchronization, which means at least one pair must be active simultaneously.

One may also ask that, given the presence of LEBs in the nodes, whether it would make sense to shut down the bus at some point instead of keeping the load constant. Our assumption has been that the aggregator has access to a steady power source, which can be either utility power or solar-charged battery, as we have experienced from our several deployment sites. Directly powering the nodes from an energy-harvesting device without associated energy storage will result in severe power-transmission loss. However, even with such energy storage, any attempt to shut down the power bus instead of sleep-and-charging would only leave less time to charge the LEBs. The increase in power-transmission loss due to the higher charging power will make it nearly impossible to make up for any saving by shutting down. Therefore, we do not consider the shut-down case.

5. CONCLUSIONS

This article identifies DC power distribution in a locally daisy-chained (LDC) network of embedded systems as an important topic for power management. Real-life systems ranging from underground water pipe monitoring systems to Power over Ethernet rely on DC power distribution, but designs to date have treated power-transmission loss qualitatively or by measurement at best. A main contribution of our work is a tool that can analyze DC power-transmission loss precisely for the very first time, instead of relying on the general rule of "higher voltage is better," as is the case with PoE. The accuracy of our solution has been validated by actual measurement.

Another contribution is that we use this tool to minimize power and energy losses due to transmission by introducing local energy buffers (LEB). Not only is it much more efficient by cutting the losses by over an order of magnitude, but more importantly, it results in feasible designs at much lower voltages, where traditional dynamic power management (DPM) fails on the bus due to high peak power that leads to high voltage drop, even if the supply can output unlimited current. Our tool can be valuable for design-space exploration over different LDC lengths, supply voltage levels, cable types and length with different resistance values, converter circuitry, and capacity of energy-storage elements.

REFERENCES

CHAN, C. 2002. The state of the art of electric and hybrid vehicles. *Proc. IEEE*. *90*, 2, 247–275.

CIEZKI, J. G. AND ASHTON, R. W. 2000. Selection and stability issues associated with a Navy shipboard DC zonal electric distribution system. *IEEE Trans. Power Deliv. 15,* 2, 665–669.

DEVADAS, V. AND AYDIN, H. 2010. Coordinated power management of periodic real-time tasks on chip multiprocessors. In *Proceedings of the International Green Computing Conference*.

IEEE. 2009. IEEE 802.3at standard. http://standards.ieee.org/getieee802/download/802.3at-2009.pdf/.

KIM, S. AND CHOU, P. H. 2012. Size and topology considerations for supercapacitor-based micro-solar harvesters. *IEEE Trans. Power Electron. 28,* 4, 391–402.

KIM, S., YOON, E., CHOU, P. H., AND SHINOZUKA, M. 2011. Smart wireless sensor system for lifeline health monitoring under a disaster event. In *Proceedings of the SPIE—Nondestructive Characterization for Composite Materials, Aerospace Engineering, Civil Infrastructure, and Homeland Security IV*. Vol. 7983.

NATHUJI, R. 2008. Mechanisms for coordinated power management with application to cooperative distributed systems. Ph.D. Dissertation, Georgia Institute of Technology, Allanta, GA.

RAJAPANDIAN, S., SHEPARD, K. L., HAZUCHA, P., AND KARNIK., T. 2006. High-voltage power delivery through charge recycling. *IEEE J. Solid-State Cir. 41,* 6, 1400–1410.

RICE, J. A., MECHITOV, K., SIM, S.-H., NAGAYAMA, T., JANG, S., KIM, R., SPENCER, B. F., AGHA, G., AND FUJINO, Y. 2010. Flexible smart sensor framework for autonomos structural health monitoring. *J. Smart Struct. Syst. 6,* 5–6, 423–438.

TON, M., FORTENBERY, B., AND TSCHUDI, W. 2008. DC power for improved data center efficiency. Tech. rep. Lawrence Berkeley National Laboratory Report.

WHITTLE, A. J., GIROD, L., PREIS, A., ALLEN, M., LIM, H., IQBAL, M., SRIRANGARAJAN, S., FU, C., WONG, K. J., AND GOLDSMITH, D. 2010. Waterwise@sg: A tested for continuous monitoring of the water distribution system in singapore. In *Proceedings of the 12th Water Distribution Systems Analysis Conference (WDSA'10)*.

WOLK, R. H. 1999. Fuel cells for home and hospitals. *IEEE Spectrum 36,* 5, 45–52.

YANG, B., LI, W., ZHAO, Y., AND HE, X. 2010. Design and analysis of a grid-connected photovoltaic power system. *IEEE Trans. Power Electron. 25,* 5, 992–1000.

ZAMORA, N. H. AND MARCULESCU, R. 2007. Coordinated distributed power management with video sensor networks: Analysis, simulation, and prototyping. In *Proceedings of the International Conference on Distributed Smart Cameras*.

Received March 2012; revised October 2012, January 2013; accepted February 2013